68th International Astronautical Congress (IAC), Adelaide, Australia, 25-29 September 2017.

IAC-17,C4,5,3,x38210

NUMERICAL ANALYSIS OF COMBUSTION AND REGENERATIVE COOLING IN LOX-METHANE ROCKET ENGINE

Abhishek Sharma[a*],Deepak Kumar Agarwal[b],J. C. Pisharady[c],S. Sunil Kumar[d]

[a] *Indian Space Research Organization (ISRO), India,*abhisheksharma@lpsc.gov.in
[b] *Indian Space Research Organization (ISRO), India,* dagarwal_iitk@yahoo.com
[c] *Indian Space Research Organization (ISRO), India*, jc_pisharady@lpsc.gov.in
[d]*Indian Space Research Organization (ISRO), India,*s_sunilkumar@lpsc.gov.in
**Corresponding Author*

Abstract

In recent years, LOX-Methane propellant combination has attracted lot of attention because of its various advantages compared to typical LOX-Hydrogen rocket engines. ISRO is currently envisioning a 10T class methane engine to replace existing propulsion system in its launch vehicles. Transcritical methane experience large thermodynamic and transport property variations at pseudo-critical temperature (near-critical fluid) which can significantly influence flow field and heat transfer characteristics. It is prerequisite to understand combustion and heat transfer characteristics of methane for future engine development. A numerical study is initiated to analyze combustion and regenerative cooling performance of methane in rocket engine elements. Combustion behaviour and flame characteristics of LOX/Methane in typical shear co-axial injector have been investigated using non-adiabatic flamelet approach. Chemical kinetic mechanism (16 species, 41 reactions) is incorporated to accommodate non-equilibrium effects by flame straining due to transcritical injection. A separate assessment on thermo-fluidic behaviour of transcritical methane in rectangular regenerative channel subjected to asymmetric heating is also carried out. The conservation equations are suitably solved to determine heat transfer characteristics and associated stratification effect of transcritical methane flow through channel across the critical point. Thermo-physical properties of methane in transcritical to supercritical regime are modeled utilizing Soave-Redlich-Kwong (SRK) equation of state. The effect of aspect ratio of channels is investigated to understand their influence on heat transfer performance of regenerative cooling system in in Lox-Methane engine.
Keywords: Supercritical, combustion, steady flamelet, transcritical

Nomenclature

$\bar{}$	=	averaged quantity
~	=	Favre averaged quantity
p	=	pressure
u_i	=	velocity component
ρ	=	density
H	=	total enthalpy
μ	=	molecular viscosity
μ_t	=	turbulent viscosity
k	=	turbulence kinetic energy
Pr	=	prandtl number
F_1	=	blending function
ω	=	specific dissipation rate
ν_t	=	kinematic eddy viscosity
σ_k	=	turbulent prandtl number for k
σ_ω	=	turbulent prandtl number for ω
Z	=	mixture fraction
ε	=	turbulent dissipation energy
σ_t	=	turbulent prandtl number
$\emptyset_i$	=	scalar like temperature, density and mass fraction
Z''^2	=	mixture fraction variance
R	=	Universal gas constant
P	=	absolute pressure
T	=	temperature
V	=	molar volume
a	=	coefficient to account for attraction
b	=	coefficient to account for repulsion
ω	=	acentric factor
T_c	=	critical temperature
P_c	=	critical pressure
χ	=	Scalar dissipation rate
ωi	=	species production rate
$C_{1\varepsilon}, C_{2\varepsilon}$	=	modeling constants
V_f	=	fuel stream velocity
V_o	=	oxidizer stream velocity

1. Introduction

The reusability of propulsion systems has got a considerable attention in last two decades because of enormous requirements in space applications. Liquid rocket engines are perfectly suitable for the propulsion system of reusable launch vehicles (RLV) because of high thrust, high reliability, and low cost. Liquid hydrogen (LH_2) & liquid oxygen (LOX) combination is widely utilized for rocket propulsion systems due to highest specific impulse and non-toxic clean combustion compared to other rocket fuels. However, the low density of LH_2 pose problems like larger tank volume, heavier vehicle mass, and higher aerodynamic drag. The other undesirable characteristics of LH_2, such as high production and insulation cost, difficulties of handling are significant drawbacks for LH_2–LOX propulsion system. The other propellant candidates such as kerosene and methane have been already recognized to provide advantage over hydrogen, in a way to minimize operational costs as well as overall propellant tank sizes. The simplest hydrocarbon: methane (CH_4) has some inherent advantages like higher specific impulse, and lower coking-sooting tendency compared to kerosene. In comparison to LH2, liquefied CH_4 is six times denser and require smaller storage vessel.LCH_4 is a soft-cryogen like LOX and could be easily operated under the simplified cryogenic arrangement, with less concern on insulation problems. In recent years, there is considerable interest in many aerospace research institutes for development of LCH_4/LOX propulsion system as a potential candidate for reusable rocket engine.

The combustion process in rocket engines is strongly influenced by injection pressure and temperature of reactants. In most situations, injection conditions are above the thermodynamic critical point of one or both propellants. At subcritical chamber pressures, inertial and surface tension forces lead to the formation of a heterogeneous spray of droplets and ligaments from the injecting jet [1], whereas near and above the critical point, surface tension and enthalpy of vaporization approaches zero. The interface separating the liquid and gas phase disappears and the injecting jet is regarded as a dense "gaseous jet"[2]. The abrupt change in thermodynamic properties near critical point, pose difficulties in development of appropriate mathematical model for numerical simulations. Cutrone et al [3] performed CFD analysis to evaluate the effects of different thermo-chemical modelling assumptions on the performance of a high-pressure LOX/CH_4 rocket thrust chamber. The effect of thermodynamic formulation on temperature, pressure, velocity and species flow field in thrust chamber is presented. Their work demonstrated that the error related to the utilization of the ideal gas model can be very large. A 20% over-estimation of steady-state combustor pressure and temperature was seen with respect to values computed using the real gas model. The study also showed that turbulent combustion model has a strong impact on the flame structure and flow field. Giorgi et al.[4] investigated the implementation of thermodynamically consistent real gas equation of state in ANSYS Fluent. CFD simulations were performed using different real gas EOS models to calculate physical properties of the species. Soave Redlich-Kwong and Peng Robinson real gas equation of state were used for accurate prediction of density. Comparison of flame characteristics was done with different combustion models like EDC, Eq.PDF, PDF flamelet. Research paper showed that the predicted flame shape is similar to experimental observations available in literature. Kim et al [5] has numerically investigated the effects of pressure and inlet temperature on coaxial gaseous methane/liquid oxygen turbulent jet flame under transcritical conditions. It is reported that the transcritical flame structure is drastically affected by elevating the chamber pressure or increasing the oxygen inlet temperature in terms of flame length, sudden expansion angle, and reverse flow strength. Recently Song et al [6] has done numerical simulation of coupled combustion and regenerative cooling in liquid rocket engine. Mixing and combustion processes are simulated by a non-adiabatic flamelet model. Coupled flow and heat transfer in a typical LOX/Methane regeneratively-cooled thrust chamber with multi-injector elements is studied. The numerical results including wall temperature and heat flux in thrust chamber under the influence of transcritical flames are thoroughly discussed in comparison with traditional methodologies. His methodology reveals that the circumferential distributions of hot-gas-side wall heat flux and temperature show obvious non-uniformity and have specific periods affected by the layout of multi-injector elements and cooling channels.

The first objective of present study is to develop RANS based combustion model for LOX/CH_4 engine and to optimize injector design based on numerical simulations and analytical understanding. A validated numerical methodology is developed which can be employed for multi-element injector rocket chamber. The paper presents a detailed comparison of flow and flame fields with the real gas modelled thermodynamic properties of propellants and products species for single element injector followed by 120 element thrust chamber.

A number of studies have been carried out to comprehend the fluid flow and heat transfer characteristics of methane at supercritical pressures to obtain fundamental understanding of the regenerative cooling process. Pizzarelli et al [7] performed a two-dimensional axisymmetric CFD analysis on methane

flow in a straight tube heated to near-critical conditions. Different constant wall fluxes were applied to study the parameters. The study showed that thermal stratification and heat transfer deterioration can occur in the transcritical region under a constant high wall heat flux.
Pizzarelli et al. [8] also carried out three-dimensional numerical analyses of turbulent heat transfer of cryogenic methane in rocket engine cooling channels at supercritical pressures. Methane was asymmetrically heated on one of the channel surface with an imposed constant wall temperature. The numerical study focused on the transcritical nature of the heat transfer processes. Under the operating and boundary conditions, it was shown that heat transfer capability of methane is strongly affected by the strong property variations in transcitical flow. Effects of the channel geometric aspect ratio on fluid flow and heat transfer were also studied. It was shown that at a cost of increased pressure loss, a high channel aspect ratio produces positive effect on the heat transfer process at a constant channel hydraulic diameter and a constant inlet mass flow rate.
Ruan and Meng [9] simultaneously carried out three dimensional numerical studies on turbulent convective heat transfer of cryogenic methane in rectangular engine cooling channels at supercritical pressures. A constant wall heat flux is imposed on the top channel wall. The fluid flow and heat transfer variations with changes in geometric aspect ratio, operation pressure and wall heat flux were studied in detail. Numerical results showed that heat transfer deterioration can take place in the cooling process because of the thermal stratification and large property variations across the pseudo-critical point. In view of this, a separate study on transcritical methane flow in single regenerative coolant channel is performed to study the phenomenon of thermal stratification and heat transfer deterioration. Furthermore, techniques to mitigate heat transfer deterioration by changing geometric aspect ratios are also investigated.

2. Numerical Modelling

2.1 Equation of State (EOS) and Thermodynamic Properties

Thermodynamic properties of propellants at extremely high pressure and low temperatureconditions cannot be accurately predicted with ideal gas equation of state. Real gas model should be employed to account for these abnormalities. In the present study, real gas effects are taken into account using Soave-Redlich-Kwong(SRK) Equation of State (EOS) [10]. SRK EOS is solved for molar specific volumeto calculate density.
General equation for pressure for cubic equation of state is given as:

$$P = \frac{RT}{(V-\bar{b})} - \frac{a(T)}{V(V^2+b_0)} \quad (1)$$

Where R is the ideal gas constant, P is absolute pressure; T is temperature and V the molar volume. Terms a and $\bar{b}$ are coefficients that account for attraction and repulsion effects among molecules respectively. Solving cubic equation requires various coefficients which are given as:

$$\alpha(T) = a_0\left(\frac{T_c}{T}\right)^n$$

$$a_0 = 0.42747\frac{R^2{T_c}^2}{P_c}$$

$$n = 0.4896 + 1.1735\omega + 0.475\omega^2$$

$$\bar{b} = b_0 - c_0$$

$$b_0 = \frac{0.08664RT_c}{p_c}$$

$$c_0 = \frac{RT_c}{p_c + \frac{a_0}{V_c(V_c+b_0)}} + b_0 - V_c$$

Numerous research studies have shown the applicability of SRK EOS for modelling thermo-physical properties in transcritical to supercritical conditions. Prateek et al [11] has highlighted the comparison between NIST and SRK density values at fixed pressure. Study showed the applicability of SRK EOS for combustion simulations.

2.2 Governing Equations

Favre averaged Navier-Stokes equations of mass continuity, momentum, energy are solved for turbulent combustion simulation [12], whereas suitably simplified equations are solved for regenerative channel heat transfer study.

$$\frac{\partial\bar{\rho}}{\partial t} + \frac{\partial}{\partial x_i}(\bar{\rho}\tilde{u}_i) = 0 \quad (2)$$

$$\frac{\partial}{\partial t}(\bar{\rho}\tilde{u}_i) + \frac{\partial}{\partial x_j}(\bar{\rho}\tilde{u}_i\tilde{u}_j) = -\frac{\partial\bar{p}}{\partial x_i} + \frac{\partial}{\partial x_j}\left(\bar{\tau}_{ij} - \overline{\rho u_i'' u_j''}\right) \quad (3)$$

Where $\bar{\tau}_{ij}$ is a shear stress term given by;

$$\bar{\tau}_{ij} = \mu\left(\frac{\partial\tilde{u}_i}{\partial x_j} + \frac{\partial\tilde{u}_j}{\partial x_i}\right) - \frac{2}{3}\mu\frac{\partial\tilde{u}_k}{\partial x_k}\delta_{ij} \quad (4)$$

$\overline{\rho u_i'' u_j''}$ is a Reynolds stress term given by;

$$-\overline{\rho u_i'' u_j''} = \mu_t\left(\frac{\partial\tilde{u}_i}{\partial x_j} + \frac{\partial\tilde{u}_j}{\partial x_i}\right) - \frac{2}{3}\mu_t\frac{\partial\tilde{u}_k}{\partial x_k}\delta_{ij} - \frac{2}{3}\bar{\rho}k\delta_{ij} \quad (5)$$

$$\frac{\partial}{\partial t}(\bar{\rho}\tilde{h}) + \frac{\partial}{\partial x_j}(\bar{\rho}\tilde{u}_j\tilde{h}) = \frac{\partial}{\partial x_j}\left(\Gamma_h \frac{\partial \tilde{h}}{\partial x_j}\right) + \bar{S}_h \qquad (6)$$

Where $\Gamma_h = (\mu/\sigma + \mu_t/\sigma_h)$

2.3 Turbulence Model

In both combustion and regenerative channel study, two equation SST k-ω RANS model is used for turbulence closure. SST k-ω model is widely used for industrial and research problems. The shear-stress transport (SST) k-ω model was developed by Menter[13] to effectively blend the robust and accurate formulation of k-ω model in the near-wall region, with free stream independence of k-ε model in the far field. Turbulent viscosity is redefined to account for transport of turbulent shear stress. Equations for turbulent kinetic energy and turbulent dissipation equation are given below by equation (5) and (6) respectively.

$$\frac{\partial}{\partial t}(\rho k) + u_j \frac{\partial}{\partial x_j}(\rho k) = P_k - \beta^* \rho k\omega + \frac{\partial}{\partial x_j}\left[(\nu + \sigma_k \nu_t)\frac{\partial k}{\partial x_j}\right] \qquad (7)$$

Where, $P_k = min\left(\tau_{ij}\frac{\partial u_i}{\partial x_j}, 10\beta^*\rho k\omega\right)$ which is the turbulent stress tensor term.

$$\frac{\partial}{\partial t}(\rho\omega) + u_j \frac{\partial}{\partial x_j}(\rho\omega) = \alpha S^2 - \beta\rho\omega^2 + \frac{\partial}{\partial x_j}\left[(\nu + \nu_t\sigma_\omega)\frac{\partial \omega}{\partial x_j}\right] + 2(1-F_1)\rho\sigma_{\omega 2}\frac{1}{\omega}\frac{\partial k}{\partial x_i}\frac{\partial \omega}{\partial x_i} \qquad (8)$$

Where,$F_1$is a blending function given as;

$$F_1 = tanh\left[\left(min\left(max\left(\frac{\sqrt{k}}{0.09\omega y}, \frac{500\nu}{y^2\omega}\right), \frac{4\rho\sigma_{\omega 2}k}{CD_{k\omega}y^2}\right)\right)^4\right]$$

And $CD_{k\omega}$ is a cross diffusion term given as,

$$CD_{k\omega} = max\left(2\rho\sigma_{\omega 2}\frac{1}{\omega}\frac{\partial k}{\partial x_i}\frac{\partial \omega}{\partial x_i}, 10^{-20}\right) \qquad (9)$$

2.4 Turbulent Combustion: Real-fluid flamelet model

LOX-Methane combustion is infinitely fast, where reaction rates are controlled by turbulent mixing only. The transcritical injection of propellants will create non-equilibrium effects, in which chemical kinetics has a role to play. Non-premixed PDF flamelet concept can effectively describe the interaction of chemistry with turbulence in the limit of fast reactions (large Damkholer number) considering non-equilibrium effects. In this model, turbulent flame is considered as an assembly of thin, laminar, locally one-dimensional flamelet structures present within the turbulent flow field. The combustion is assumed to occur in thin sheets with inner structure called flamelets [14]. Mixing rate for a non-premixed combustion problem can be described by a conserved scalar known as mixture fraction. For a two feed system, mixture fraction is given by:

$$z = \frac{m_i - m_{i,ox}}{m_{i,fuel} - m_{i,ox}} \qquad (10)$$

Where $m_{i,fuel}$ and $m_{i,ox}$ is the species mass fraction at the fuel and oxidizer inlet respectively. The value of z varies from 1 in fuel stream to 0 in oxidizer stream and z is independent of chemistry and hence there is no source term in its governing equation. The whole combustion process is simplified to mixing problem. The laminar diffusion flame equations can be transformed from physical space to mixture fraction space[15]. The mixture fraction Z is assumed to be given in the flow field as a function of space and time

$$\rho\frac{\partial Z}{\partial t} + \rho V.\nabla Z = \nabla.(\rho D \nabla Z) \qquad (11)$$

In turbulent combustion, instead of instantaneous flame location, mean quantities such as Favre mean mixture fraction equation is calculated by

$$\bar{\rho}\frac{\partial \tilde{Z}}{\partial t} + \bar{\rho}\bar{V}.\nabla\tilde{Z} = \nabla.\left(\bar{\rho}D_t\nabla\tilde{Z}\right) \qquad (12)$$

Turbulence-chemistry interaction is accounted by using transport equation for mixture fraction variance which is given as:

$$\bar{\rho}\frac{\partial \widetilde{Z''^2}}{\partial t} + \bar{\rho}\bar{V}.\nabla\widetilde{Z''^2} = \nabla.\left(\bar{\rho}D_t\nabla\widetilde{Z''^2}\right) + 2\bar{\rho}D_t(\nabla\tilde{Z})^2 - \bar{\rho}\tilde{\chi} \qquad (13)$$

Here $\tilde{\chi}$ is the mean scalar dissipation rate, representing the non-equilibrium effects caused by straining of flames in transcritical combustion region. It is modeled as:

$$\tilde{\chi} = C_\chi \frac{\tilde{\varepsilon}}{\tilde{k}}\widetilde{Z''^2} \qquad (14)$$

Combustion occurs in a thin layer in the vicinity of this surface, if the local mixture fraction gradient is sufficiently high. The turbulent flame brush is modelled with the value of $\tilde{\chi}$ at stoichiometric conditions ie$\tilde{\chi} = \tilde{\chi}_{st}$.In the limit $\tilde{\chi} \to 0$ the reaction tends to equilibrium and the increase in $\tilde{\chi}$indicates the non-equilibrium effects. For time independent adiabatic systems, the flamelet equations including one equation of temperature and n equations of the species mass fractions are given as follows:

$$\rho C_p \frac{\tilde{\chi}_{st}}{2}\frac{\partial^2 T}{\partial Z^2} = \sum_{i=1}^{n} h_i \dot{\omega}_i \qquad (15)$$

$$-\rho \frac{\tilde{\chi}_{st}}{2} \frac{\partial^2 Y_i}{\partial Z^2} = \dot{\omega}_i \qquad (16)$$

The main advantage of the flamelet model is that even though detailed information of molecular transport processes and chemical kinetic are incorporated, the numerical resolution of small length and time scales is not necessary. This makes the method very robust and helps to avoids problems of solving highly nonlinear kinetics in turbulent flow field. A skeletal model (SK) was employed to model methane-oxygen finite-rate chemical reactions in this study which is obtained from the Grimech 3.0 [16] through a reduction of the more detailed mechanism.
Instantaneous scalar quantities like temperature, density and mass fractions of species are function of instantaneous mixture fraction and can be calculated as

$$\emptyset_i = \emptyset_i(z) \qquad (17)$$

2.5 Probability Density Function

In non-premixed combustion problem, under the assumption of infinitely fast chemistry, equilibrium solution relates all reactive scalars to mixture fraction. The easiest way to obtain these scalars is to assume a probability density function. Because of the assumption that a turbulent flame brush is an assembly of separate diffusion flamelets, turbulent flame mean scalars can be calculated by the probability density function (PDF) of Z and $\tilde{\chi}_{st}$.

$$\bar{\emptyset}_i = \iint \emptyset_i(Z, \tilde{\chi}_{st}) p(Z, \tilde{\chi}_{st}) dZ \, d\tilde{\chi}_{st} \qquad (18)$$

3. Results & Discussion

3.1 Lox-Methane Combustion Study

3.1.1 Validation study

A validation study is performed initially in a simplified two-dimensional axi-symmetric domain, in accordance with domain used by Kim et al. [5]. Figure 1 shows the computational domain and boundary conditions for the RCM-3(V04)[17]test case. Numerical methodology is verified by comparing the obtained flame shape/temperature contours with Kim et al [5] study. Numerical results with steady flamelet model showed good qualitative agreement with results from literature, in terms of flame length and shape. The slight difference in LOX core length and maximum temperature obtained is attributed to difference in kinetic mechanism used for flamelet generation. The validated methodology has been used for all further reported analysis.

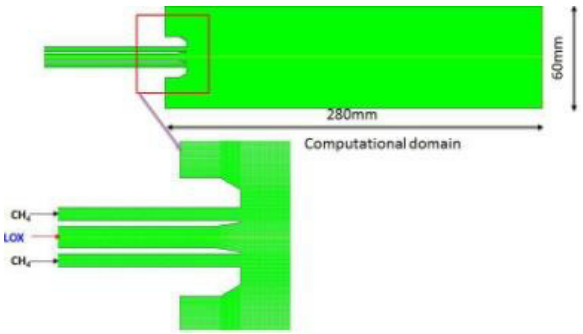

Fig.1: Computational Domain for Validation Study

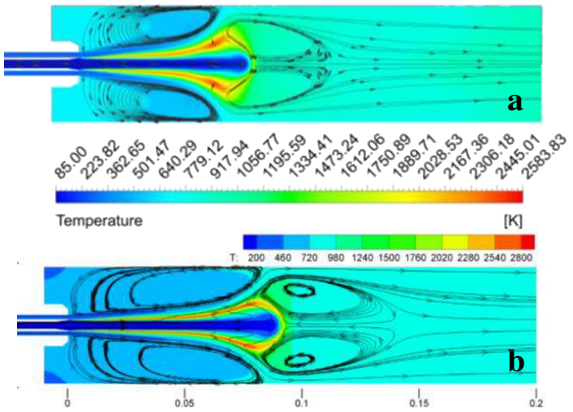

Fig.2: Temperature Comparison: Simulated (a) to Literature [5] (b)

3.1.2 Parametric Study: Single Element Injector

A parametric study on single element injector using two-dimensional axi-symmetric domain is carried out to understand the effect of injection and geometric conditions. Reactive flow simulation for a simple shear co-axial single injector element is carried out initially followed by different velocity ratio and recess length of LOX post. The effects of Velocity Ratio (V_f/V_o) and LOX post recess length on combustion behaviour and flame shape has been numerically investigated. Total 6 cases are performed, 3 cases for different velocity ratio (VR)and 3 cases for different LOX post recess length on VR=15.The mass flow rates of propellants and LOX velocity is kept constant for all cases

Figure 3 shows computational domain which includes injector ducts and part of combustion chamber. The domain extends downstream of the injector face plate up to a length of 500mm and has radius of 150mm. A very fine grid near the LOX post is used to capture the density variation accurately. LOX is introduced through inner duct at 85K and methane is introduced from annular duct at 350K.The results for the six cases have been discussed and various observations were made regarding the flow and flame structures.

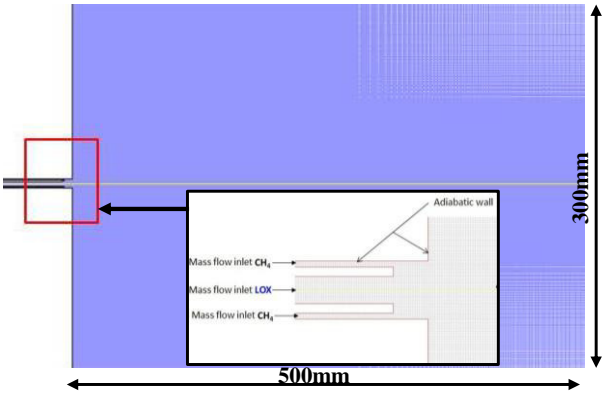

Fig.3: Computational domain & Injector area

3.1.3 Temperature and Flame zone contours

The temperature contours for 6 cases is shown together in Fig.4.Temperature contour shows that the case 6 (VR:15, 1.5dRecess) has shortest flame length, which indicates fast consumption of LOX core. The potential LOX length is also seen to be smaller than other cases. The flame is seen to propagate through shear layer and is anchored at recess portion. The prime aim of these test cases was to reduce flame length without compromising the flame temperature. A shorter combustion chamber is sufficient for a shorter flame length, so the overall size and the cost of production can be reduced.

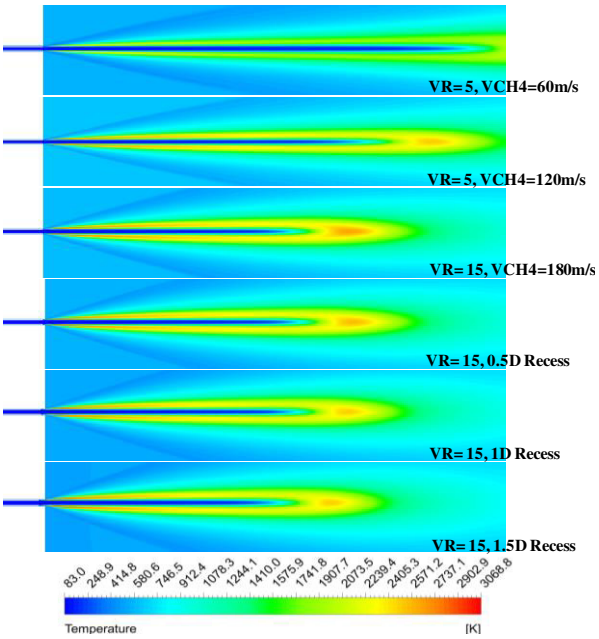

Fig.4: Temperature and Flame zone contours for the parametric study cases

The adiabatic flame temperature for LOX/methane at 60bar is approximately 3400K. The maximum temperature obtained for the case 6 is 2454K. The difference in value is because of shift from equilibrium due to the straining of flame in the transcritical region. The reduction in peak temperature is only a marginal but the flame length reduction is significant for case 6, even though same mass flow rate of propellants are used for all six cases.

Figure5 shows the plot for mixture fraction and temperature the axis of injector. Highest flame temperature is achieved for mixture fraction of 0.32 which is slightly higher than the stoichiometric mean mixture fraction (0.22). The reason for such deviation can be attributed to non-equilibrium effects of flame straining.

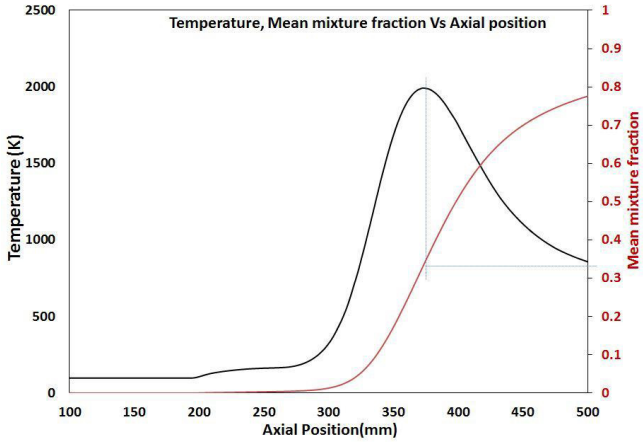

Fig.5: Temperature variations with mixture fraction along axis

Parametric analysis for single element injector showed that the case 6 (VR:15, 1.5d Recess) is the most efficient case with lowest LOX core length, highest turbulence mixing and a well-developed flame zone compared to the other cases. The study further validates the methodology used for transcritical injection and turbulent combustion in single element domain. Based on this study, case 6 injection and geometric conditions were finalized to be employed for multiple injector element 3D reactive flow simulation.

3.1.4 Lox-Methane Thrust Chamber 3D Simulation

A three dimensional reactive flow simulation is carried out for 10T LOX-Methane thrust chamber, to understand combustion process in a multi injector configuration. The injector head consisted of 120 shear co-axial injector elements as shown in Figure 6(a). The injector elements on the face plate are arranged in 4 circular rows with a symmetric order which is shown in figure 6(b).

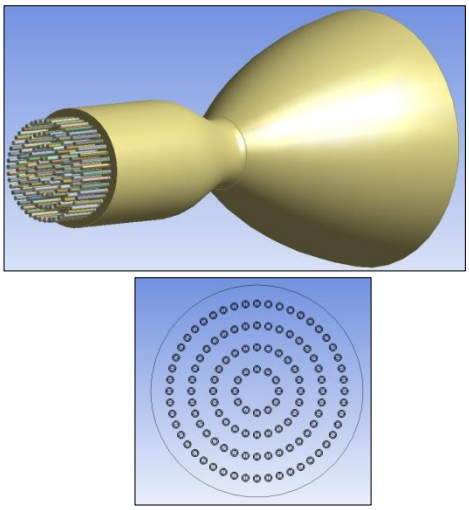

Fig. 6: Chamber actual geometry& Injector arrangement

The advantage of symmetry in circumferential direction was taken to conduct analysis for only 30° sector. The computational domain with boundary conditions is shown in figure 7. A close up shot of computational domain and a single injector element is also shown. The oxidizer stream is injected at a temperature of 85 K, while the fuel stream is injected at a temperature of 350 K.

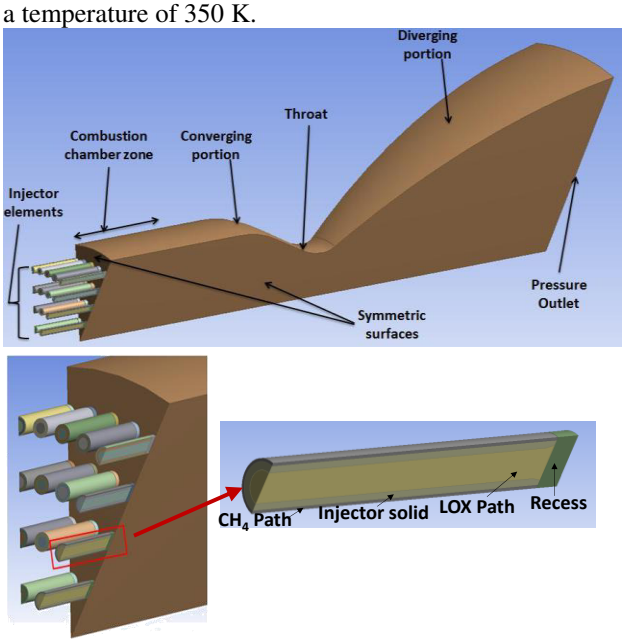

Fig. 7: 3D Computational domain & Injector details

Initial calculations are performed by applying the overall oxidizer-to-fuel mixture ratio O/F = 3.5 and combustion chamber pressure of 6MPa. The inlet boundary condition is given as "mass flow inlet" and outlet is fixed as "pressure outlet". No slip boundary condition is employed for all wall surfaces. Symmetry condition is used for left and right symmetric surfaces.

3.1.4.1 Simulated Density fields

Figure 8 shows the close up view of density contour near to the injection region. The density prediction for both LOX and methane is accurate with SRK EOS model. A drastic reduction in LOX density has been seen after the injection because of the rapid LOX core consumption. Since the combustion started right after the fuel post, there is a huge temperature rise which causes the change in density. A general trend of drop in density with increase in temperature is observed from the start of combustion from the fuel post.

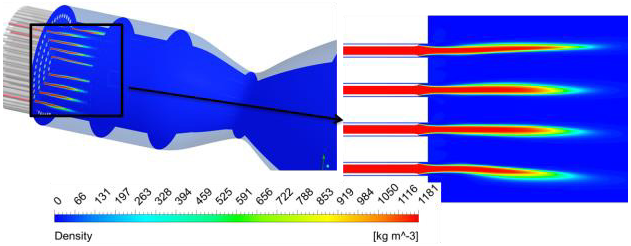

Fig. 8: Density contours in 3D domain and in Y-Y plane

3.1.4.2 Temperature Distribution in Chamber

Figure 9 depicts the computed static temperature contour of hot gas in LOX/Methane multi injector thrust chamber. It shows that, the development of flame is completed in the middle of cylindrical part of chamber. In the divergent portion, flames start to blend into each other and hot gas tends to be more homogeneous. Figure 10 shows the details of flame shape and structure at Y cross- section cut plane. It shows flame to anchor at LOX post and mix together as they reach nozzle throat. It shows that the flames from intermediate row of elements are constrained by hot gases from the outer row as well as from inner row of elements.

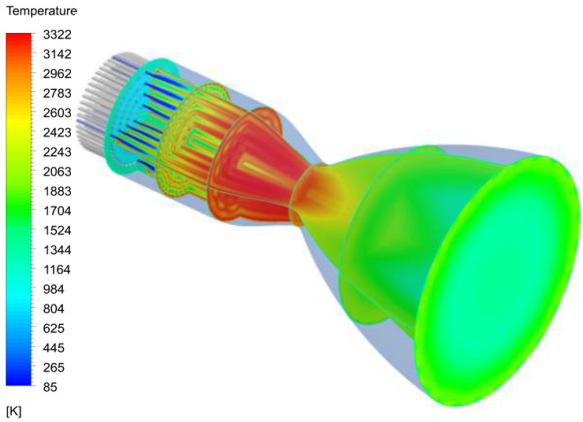

Fig.9: Temperature contours of hot gas in the thrust chamber

The intermediate row of elements display effective heat exchange to the LOX core. The LOX core length for intermediate row elements is seen to be comparatively lesser than the outer row and inner row elements. A rapid expansion of flames attached to outer injector elements was seen, which is caused by dramatic increase of oxygen temperature. The radial expansion of flames will have an impact on combustion chamber wall from heat transfer aspect.

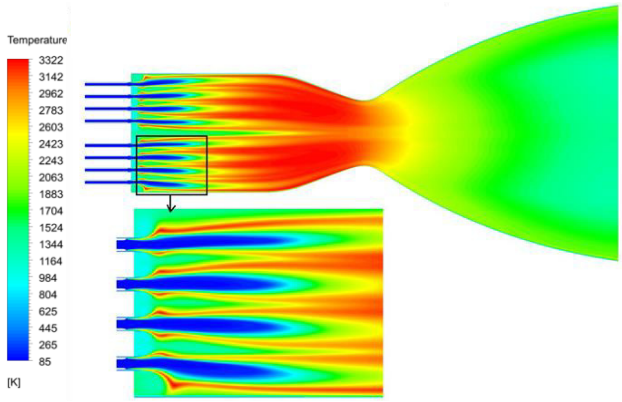

Fig.10: Temperature contours of hot gas in the thrust chamber in Y-Y plane

3.1.4.3 *Velocity and Mach Number*

Hot gases from the combustion chamber are accelerated through the C-D nozzle. The velocity and Mach number contours are shown in Fig 11. The hot gases blend together up to throat region and accelerate in the diverging section. Mach contour shows subsonic flow in the convergent zone and supersonic after the throat. The maximum Mach number obtained is 3.61, which is in close match with NASA CEA calculations.

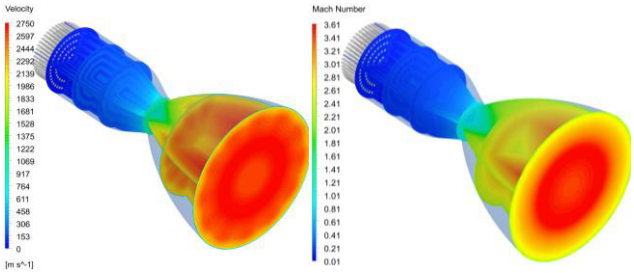

Fig. 11: Velocity & Mach Number Contour in thrust chamber

3.1.4.4 Species Concentration

The combustion characteristics in this domain are assessed by concentration of mass fraction for LOX, methane and burnt products. Figure 12 shows the mass fractions of propellants downstream of the combustion chamber. The negligible presence of LOX & methane in divergent section indicates the efficient combustion of propellant early in the cylindrical section.

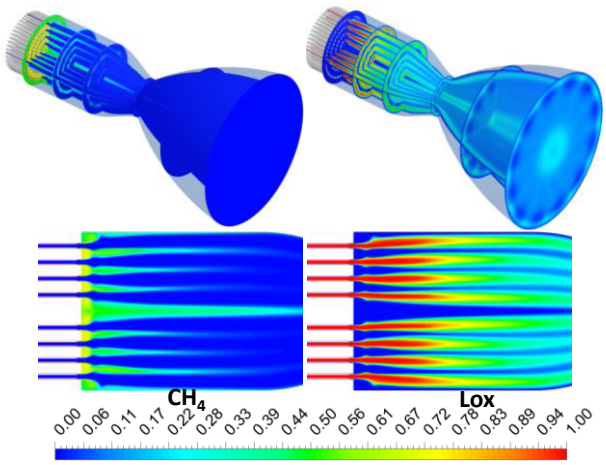

Fig. 12: Mass fraction of Methane & LOX in Chamber& near view

The near view shot of propellants mass fractions shows high CH_4 mass fraction and low O_2 mass fraction at centre, which has led to insufficient combustion at axial location. This is happening due to arrangement of injector elements on face plate as shown in Fig.6. This can be overcome by altering the injector configuration or by providing more LOX through inner most rows of injection elements. The concentration of major product species H_2O and CO_2 in chamber is monitored to assess combustion efficacy. The mass fraction of $H_2O$and CO_2 at chamber cut plane is shown in Fig.13.

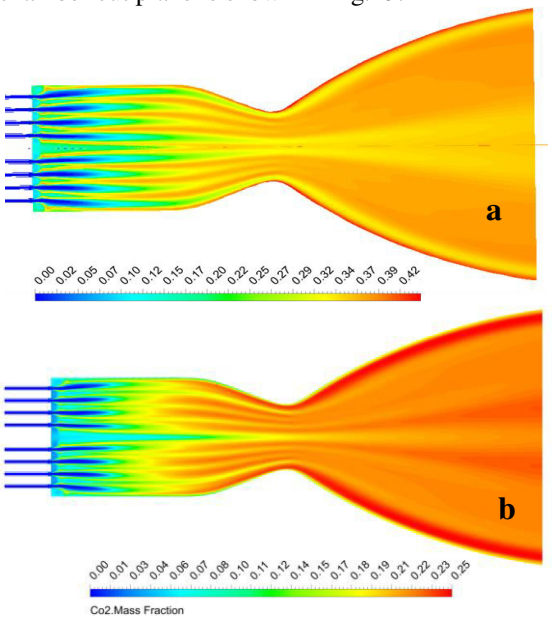

Fig. 13: Mass fraction of H_2O(a) & CO_2 (b) at chamber cut plane

H_2O mass fraction shows uniform combustion in chamber with concentration close to stoichiometry, whereas CO_2 mass fraction in the shear layer is low compared to a stoichiometric condition. The low value

of CO_2 mass fraction is attributed to presence of some unburned propellants and dissociation of CO_2 into other species.

The three dimensional study showed that the combustion methodology finalized based on validation study and parametric variations in single element injector can be employed to understand combustion characteristics of multi-injector Lox-methane combustion chamber. The steady flamelet methodology incorporating the non-equilibrium effects has been successfully implemented. The gas temperature and Mach pattern in Lox-methane chamber is observed to be in close match with analytical calculations.

3.2 Lox-Methane Regenerative Channel Study

A simplified study is carried out to simulate the flow of transcritical methane and associated heat transfer aspects in a single coolant channel. In a typical rocket engine cycle, methane will enter the channel at sub-critical temperature and above critical pressure. The adverse effects of transcritical inlet conditions have been discussed in detail by Pizzarelli [7] and others as discussed in section 1.

Figure14 shows the computational domain used for analysis, with boundary conditions as highlighted. Mass flow inlet condition was imposed on methane inlet, with chamber inner wall fixed at variable heat flux calculated based on Bartz equation [18]. Methane flows in counter-flow direction in respect to flow in chamber. Governing equations and thermo physical properties are modeled, as mentioned in section 2. The governing equations were solved to determine the heat transfer characteristics of transcritical methane flow in channel.

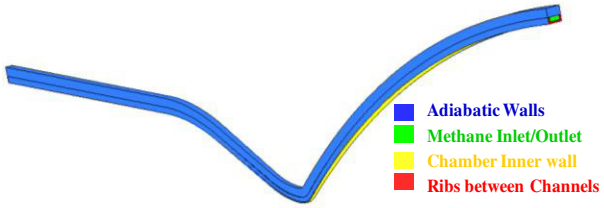

Fig. 14: Channel geometry and boundary conditions

Figure 15 shows the temperature variation over the inner surface of chamber wall. It shows a peak temperature of 1998K at the divergent location of chamber. The axial variation of wall temperature is displayed in Fig.15.

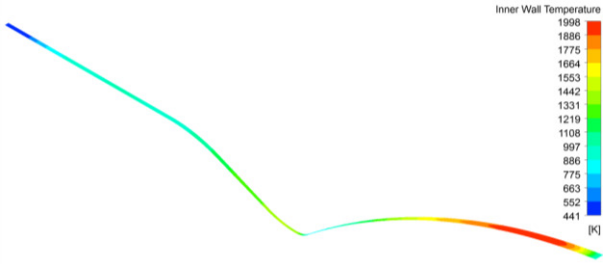

Fig. 15: Coolant channel wall temperature contour

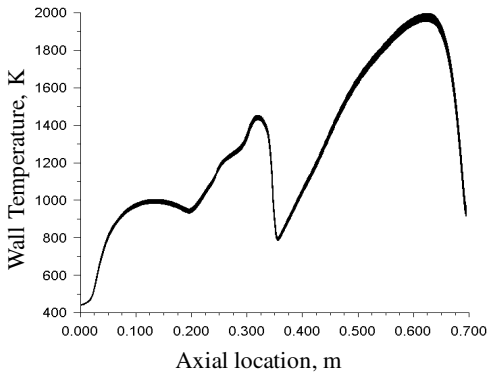

Fig. 16: Channel wall temperature variation

It is evident from Figure 15 &16 that greater wall temperature is observed in the cooling channel during transcritical methane flow. The phenomenon of thermal stratification and heat transfer deterioration as observed in literature (Pizzarelli et al [7]) is observed clearly in temperature contours. Due to separation of fluids based on density, a two different fluid regions- gas like and liquid like exist in the same plane. The presence of high specific heat region in between the fluid inhibits the heat transfer and causes the phenomenon of heat transfer deterioration. Figure 17 displays specific heat (C_p) variation at planes over the divergent section of channel every 40mm starting from inlet.

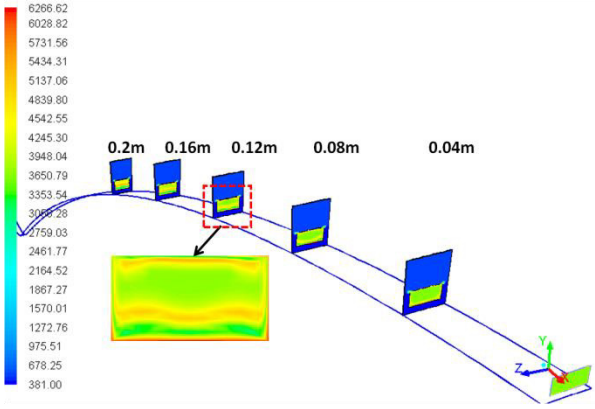

Fig.17: Contours of specific heat (J/kg-k) showing stratification

The Cp distribution at plane 0.12m clearly shows a formation of higher Cp zone in between away from wall, which behaves as a barrier to heat transfer and has led to high temperature (Fig.15) at divergent section.

3.2.1 Heat Transfer Enhancement by Division of Channels

In order to avoid property stratification and resultant heat transfer deterioration in channel, a study on division of channels into two up to throat region is carried out. The channel divisions are basically bifurcations to increase the channel geometric aspect ratio in heat transfer affected region. Fig.18 shows the domain used for this study.

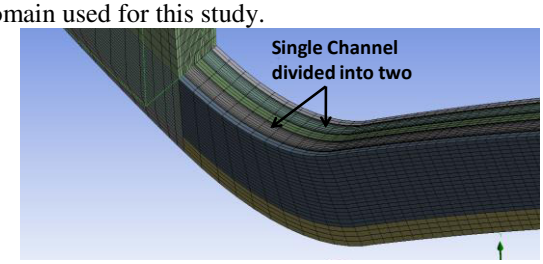

Fig.18: Domain of divided channels

The heat transfer characteristics in increased aspect ratio channels are evaluated for possible advantage over single channel configuration. Figure 19 displays temperature map of divided channel configuration. The maximum wall temperature observed on inner wall is seen to reduce to 977K in comparison to 1998K as was observed in undivided channel configuration. The maximum wall temperature is seen at throat location unlike at the divergent section of channel captured earlier. The temperature of divergent section is seen to reduce significantly and is within safe operating limits. Figure 20 shows the variation of wall temperature along the length of channel.

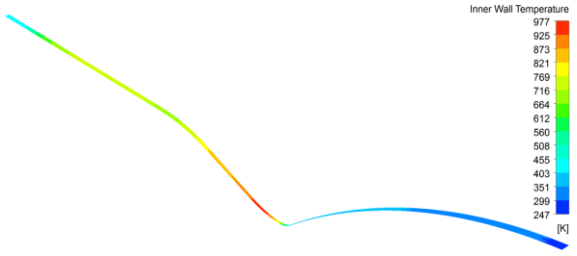

Fig. 19: Coolant channel wall temperature contour

A significant change in chamber wall temperature is noticed in divided channel configuration. The larger heat transfer due to enhanced turbulent mixing in divided channel configuration avoided the property stratification and resultant high temperature in divergent section of channel. The high velocity methane flow in divided channels has also led to lower temperature at throat section of channel.

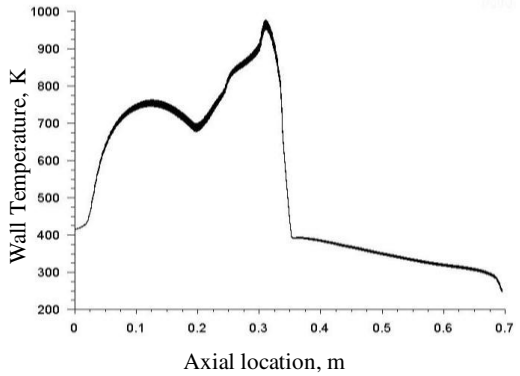

Fig. 20: Channel wall temperature variation

A simplified study has been done to understand heat transfer effects due to large property variation of methane near pseudo-critical temperature. A divided channel study performed to mitigate heat transfer deterioration and resultant high temperature showed good promise. The improvised design based on CFD simulations can be implemented for further optimization of rocket channel design.

4. Conclusion

Supercritical combustion of Liquid oxygen and Methane has been modelled numerically using steady flamelet combustion methodology. The numerical models adopted for combustion and turbulence closure are validated using results obtained from Mascotte Chamber RCM-3(V04) test case. SRK Real gas equation of state has been successfully implemented for predicting density of the propellants at high pressure conditions. A parametric study (2D case) is conducted to study the effect of injection velocity ratio and LOX post recess length on combustion behaviour and flame shape. A 3D reactive flow simulation is carried out for a typical thrust chamber of 10T LOX-Methane engine. Results showed that, the validated methodology can be successfully implemented on 120 element full thrust chamber. The overall flow characteristics in full chamber simulation matched closely with NASA CEA results. A separate study on flow of transcritical methane in coolant channel was also done to capture heat transfer deterioration due to stratification effects. A technique to improve the heat transfer characteristics in coolant channel is also analysed. The division of channel up to throat location in order to increase aspect ratio is found to produce good overall effect and can be implemented for Lox-Methane engine channel design.

5. References

[1]. Oefelein .J. C and Vigor Yang. Modeling high-pressure mixing and combustion processes in liquid rocket engines. J. Propul. Power, 14, 1998.

[2]. Mayer W., Telaar R., Branam .J, Hussong .J, and Raman. Measurements of cryo-genic injection at supercritical pressure. International journal of Heat Mass Transfer, 39:709{719, 2003.

[3]. Cutrone .L, Battista, and Ranuzzi. Supercritical high pressure combustion simulation for lox/ch4 rocket propulsion systems. American Institute of Aeronautics and Astronautics, 2008.

[4]. Giorgi M.G, Sciolti, and Ficarella .A. Application and comparison of di erent com-bustion models of high pressure lox/ch4 jet ames. American Institute of Aeronautics and Astronautics, 2011.

[5]. Taehoon Kim, Yongmo Kim, and Seong-Ku Kim. Effects of pressure and inlet temperature on coaxial gaseous methane/liquid oxygen turbulent jet flame under trans-critical conditions. The Journal of Supercritical Fluids, 81:164,174, 2013.

[6]. Jiawen Song and Bing Sun. Coupled numerical simulation of combustion and regenerative cooling in lox/methane rocket engines. Applied Thermal Engineering, 2016.

[7]. Marco Pizzarelli, Francesco Nasuti, Marcello Onofri, 'CFD analysis of transcritical methane in rocket engine cooling channels', Journal of Supercritical Fluids 62 (2012) 79– 87

[8]. Marco Pizzarelli, Francesco Nasut, and Marcello Onofri, 'CFD Analysis of Curved Cooling Channel Flow and Heat Transfer in Rocket Engines', 46th AIAA/ASME/SAE/ASEE Joint Propulsion Conference & Exhibit, 25 - 28 July 2010, Nashville, TN

[9]. Bo Ruan and Hua Meng. "Supercritical Heat Transfer of Cryogenic-Propellant Methane in Rectangular Engine Cooling Channels", Journal of Thermophysics and Heat Transfer, Vol. 26, No. 2 (2012), pp. 313-321

[10]. Soave and Giorgio. Equilibrium constants from a modied redlich-kwong equation of state. Chemical Engineering Science, 27(6):1197{1203, 1972.

[11]. Prateek Garg, Abhishek Sharma, Deepak K. Agarwal, and Mohan Varma. "Numerical Modeling of Liquid Oxygen and Kerosene Combustion at High Pressures", 55th AIAA Aerospace Sciences Meeting, AIAA SciTech Forum, (AIAA 2017-2023)

[12]. ANSYS FLUENT v.16 Registered

[13]. Menter, Kuntz, and Langtry. Ten years of industrial experience with the sst turbulence model. Turbulence, heat and mass transfer, 4(1):625{632, 2003

[14]. Peters and Norbert. Turbulent combustion. Cambridge university press, 2000.

[15]. Stephen R Turns et al. An introduction to combustion, volume 287. McGraw-hill New York, 1996.

[16]. Singla G, Scouaire P, Rolon C.C.S, Zurbach S, and Thomas J. Experiments and simulations of lox/ch4 combustion at high pressures. Proc. Combust. Inst, 30:2921{ 2928, 2005

[17]. Minotti and Bruno. Comparison between simulations of real and ideal lre combustion of lo2-ch4. Recent Patents on Space Technology, 2:1{9, 2010.

[18]. D.R. Bartz, A simple equation for rapid estimation of rocket nozzle convective heat transfer coefficients, Technical notes, DA-04-495, California Institute of Technology, 1957

.